ELSEVIER

Journal of Molecular Catalysis A: Chemical 166 (2001) 123–134

JOURNAL OF MOLECULAR CATALYSIS A: CHEMICAL

www.elsevier.com/locate/molcata

Design of microporous transition metal oxide catalysts and investigation of their synthesis conditions

F. Corà [a,*], C.R.A. Catlow [a], D.W. Lewis [b]

[a] *Davy-Faraday Research Laboratory, The Royal Institution of Great Britain, 21 Albemarle Street, London W1X 4BS, UK*
[b] *Department of Chemistry, University College London, 20 Gordon Street, London WC1H 0AJ, UK*

Abstract

Microporous materials based on cations of medium acidic strength, such as the alumino-silicate zeolites, represent one of the most widely used heterogeneous catalysts. Synthesising novel materials that could combine the molecular-sieve characteristics of Si-zeolites, with the much higher acidic strength and redox properties of early transition metal cations, would be a major breakthrough in catalysis. In this paper we examine this topic employing computer modelling in advance of experiment: we design suitable microporous structures of MoO_3 and WO_3, compare their relative energy with those of the known dense polymorphs of the materials, and finally explore the possibility of their synthesis via a template/host approach previously developed for zeolitic materials.

Keywords: Microporous materials; Alumino-silicate zeolites; Heterogeneous catalysts; Transition metal oxides

1. Introduction

The crystalline oxides of Mo^{6+} and W^{6+} ions, built up as a network of connecting MO_6 octahedral units, are at the basis of a rich solid state chemistry, which comprises several phases and polymorphs. Because of the high O/M ratio, the binary oxides MoO_3 and WO_3 contain empty interstices in the oxygen sublattice, where external species can be reversibly accommodated to form the insertion compounds, or bronzes, A_xMO_3. The latter can be described as composed of an MO_3 framework, in whose interstices are located the inserted, or extraframework species, A.

The properties of the Mo and W trioxides and bronzes are exploited in a diverse range of applications, including gas-sensors [1], catalysis [2,3], electrochromic devices [4,5] and solar cells [6]. The insertion process that leads to the formation of the bronzes, in particular, can be exploited in two ways: once the host MO_3 framework is formed, the intercalation of extraframework ions can be driven electrochemically, and employed either to store energy in rechargeable batteries [7,8], or to modify the physical properties of the MO_3 host, as in electrochromic devices [4,5]. On the other hand, the presence of extraframework ions during the synthesis of the MO_3 host, can be used to stabilise different polymorphic structures of the forming MO_3 backbone.

In the paper we focus on the latter topic, employing computer modelling to investigate the feasibility of the synthesis of microporous frameworks of MoO_3 and WO_3. Although the method is applied to structures with composition MO_3, the procedure employed and most of the results have general validity, and can be extended to the whole class of early transition metal oxides.

* Corresponding author.
E-mail address: furio@ri.ac.uk (F. Corà).

1381-1169/01/$ – see front matter
PII: S1381-1169(00)00465-9

We first present an overview of the calculations performed and of the existing polymorphic structures of the Mo and W trioxides and bronzes; we then design new microporous structures, and examine their relative stability and the feasibility of their synthesis.

2. Computational details

The crystalline oxides are described with periodic boundary conditions, at the ab initio Hartree-Fock (HF) level of approximation, as implemented in the computer program CRYSTAL [9,10].

The wavefunction of the solid is obtained as a linear combination of localised functions, or atomic orbitals, associated with the constituent atoms. The basis sets employed to describe the Mo and W ions are composed of an effective core pseudopotential of the Hay-Wadt type [11], coupled with a split-valence set of basis functions for the valence electrons. Their derivation and performance can be found in [12,13].

Numerical approximations are introduced in the evaluation of the Coulomb and exchange series for infinite systems. In the CRYSTAL code, the accuracy is controlled by a set of "cut-off" tolerances (see [10] for details); the values we have chosen (8, 7, 8, 8, 16) reduce the effect of numerical inaccuracies to a minimum.

Reciprocal space integrals are performed as a weighted sum at a discrete set of *k*-points, whose number is chosen in such a way that the results of the numerical integration are converged to within 10^{-4} Hartree for the total energy and $10^{-5}|e|$ for the Mulliken charges. This corresponds to an $8 \times 8 \times 8$ sampling of the first Brillouin Zone for the perovskite polymorph, and has been scaled in the other structures according to the lattice parameters.

Geometry optimisations have been performed with a numerical conjugated-gradient procedure, stopped when the energy difference at subsequent cycles had fallen below 10^{-6} Hartrees.

3. Known polymorphs of the Mo and W trioxides and bronzes

Among the known structural types of the Mo and W trioxides and bronzes, four are of direct relevance to investigate the effect of extraframework ions during the synthesis; these are the perovskite (PV), layered (L), hexagonal (Hex) and pyrochlore (PY) polymorphs, shown in Fig. 1. The M–O framework in all four structures has stoichiometry MO_3.

The thermodynamically stable phase of WO_3 at ambient conditions is a distorted PV structure [14–19], which is metastable in MoO_3 [20,21]. The stable phase of MoO_3 is instead the L polymorph, or α-MoO_3 [22–24], not displayed by WO_3. A metastable hexagonal form has been synthesized for both WO_3 [25–29] and MoO_3 [30–33], while a polymorph isostructural to the octahedral backbone of the mineral pyrochlore, $Ca_2Nb_2O_7$, has recently been observed for WO_3 [34–36], but not for MoO_3.

The relative order of stability of the four polymorphs in the bronzes is different. In the W bronze family, the PV polymorph is stable for small inserted atoms (H, Li, Na) [37–39], while larger atoms or groups of atoms (K, Cs, Rb, In, NH_4) favour the Hex structure [40–42]. Inserted atoms which are even larger (Tl, Cs, Rb) stabilise the PY structure [34–36], depending also on the synthesis conditions [43–45]. Examining the structural stability in the MoO_3 family, we see instead that MoO_3 is layered, Na_xMoO_3 is a cubic perovskite [46], while K_xMoO_3 and the bronzes of larger inserted atoms are stable in different layered forms (see [47] and references therein).

To understand the effect of the extraframework ions on the phase stability, it is instructive to examine the structure of the four polymorphs, and the characteristics of their interstices.

The MO_3 framework of PV, Hex and PY structures is based on corner-sharing only of MO_6 octahedra. In PV materials, octahedra form four-membered rings in each of the crystallographic planes; interstices are located in the dodecahedral sites (A) of the O sublattice. The Hex structure is instead composed of alternating three- and six-membered rings of octahedra in the *ab* plane; this arrangement is repeated along *c*, leaving a set of parallel triangular and hexagonal channels, of which only the hexagonal is large enough to host inserted species.

In the PY structure, six-membered rings of octahedra are oriented along the $< 1\,1\,1 >$ directions of the cubic unit cell, creating a three-dimensional network of interconnecting hexagonal channels. Finally, in the L polymorph, MO_6 octahedra connect

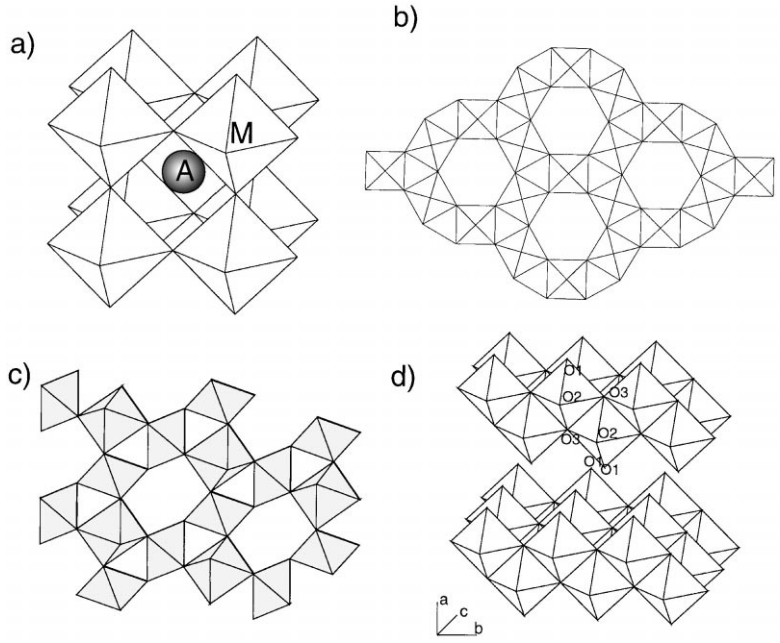

Fig. 1. Connectivity of the MO_6 octahedra in the MO_3 framework of Mo and W trioxide and bronzes: (a) PV; (b) Hex; (c) PY; (d) L polymorphs.

corner- and edge-sharing in the *bc* crystallographic plane, leaving a layered structure in the perpendicular direction, *a*. Interstices are available in the interlayer region.

The four polymorphs examined have a different number of interstitial sites, and of different dimensions. In the three corner-sharing arrangements (PV, Hex and PY), for instance, the size of the vacant interstices increases in the order of PV < Hex < PY, which is obviously an important feature of the host framework in insertion processes.

4. Framework stability

The insertion reaction that leads from the binary oxides to the bronzes

$$MO_3 + x(A^+ + e^-) \rightleftharpoons A_xMO_3 \quad (1)$$

can be formally decomposed into two steps: the extraframework species A ionise upon insertion, and cede their valence electrons to the host MO_3 framework, reducing the transition metal ions M; in a band-structure description of the solid, the extra electrons fill the energy states at the bottom of the conduction band (CB). At the same time, the ionised A^+ particles occupy in cationic form the empty interstices of the host framework.

Both components of the insertion process, the added electrons and the inserted cations, can induce structural strains in the host transition metal oxide. In our recent work, we have examined them separately with computer modelling. In particular, we have shown that the CB electrons modify the stability of structural distortions which involve M off-centerings in its coordination octahedron [48,49]. In the PV structure, for instance, the M off-centering hybridises a set of levels which are M–O non-bonding in the cubic phase into a pair of M–O bonding (in the valence band, VB) and M–O antibonding (in the CB) crystalline orbitals. When M has the formal electronic configuration $d^{(0)}$, as in MoO_3 and WO_3, only the M–O bonding level in the VB is filled, and the distortion is stable; if instead the M–O antibonding orbital in the CB is occupied, as in the bronzes A_xMO_3, its population opposes the distortion [48,49]. This finding is in agreement with the experimental evidence concerning the structure of MoO_3, WO_3 and of their sodium bronzes $NaMO_3$.

The same M–O bonding pattern described above occurs in the other polymorphs examined [50], and the finding that the population of CB states in the bronzes opposes M off-centerings has general validity.

The relative stability of the host MO_3 framework in the binary oxides and in the bronzes can therefore, be obtained by two separate sets of calculations, in which the structure of the MO_3 backbone is optimised without constraints (CB empty) or under the constraint of having M on-centre in its coordination octahedron (CB partially populated). The results of our HF calculations are summarised in Table 1. We note, in particular, that the undistorted L polymorph of MoO_3 is unstable compared to the other polymorphs examined, suggesting that bronzes based on L-MoO_3 would not be structurally stable following insertion; this is due to the very high energy gained in optimising the distance of the short Mo–O_1 bonds of Mo with the 1-coordinate, outermost O ions in the layers [12]. The population of the Mo–O_1 antibonding level which occurs in the bronzes destabilises the L polymorph. The relative stability of the other three polymorphs, parallels instead their relative density, as higher electrostatic energies stabilise the densest structures; in WO_3, for instance, the Madelung field (measured as the difference of electrostatic potential in the W and O sites) is highest in the PV polymorph, while in the Hex and PY it is respectively 0.125 and 0.365 V less favourable. The latter data are roughly proportional to the energy difference between the polymorphs.

Table 1
Calculated energies for the MO_3 framework structures examined[a]

Polymorph	ΔE (eV)	
	MoO_3	WO_3
Fully optimised		
PV	0.000	0.000
Hex	–	0.454
PY	0.957	1.524
L	−0.006	–
Optimised with M on-centre		
PV	0.000	0.000
Hex	0.239	0.318
PY	0.561	0.725
L	4.281	5.471
$PV^{2\times1}$	–	0.736
$PV^{2\times2}$	0.962	1.634
$H^{2\times1}$	0.524	0.902
$H^{2\times2}$	1.128	1.393

[a] ΔE is the relative energy, in eV per MO_3 formula unit, with respect to the PV polymorph. The upper part of the table refers to the fully optimised phase of each polymorph, and applies to the relative stability of the binary oxides MoO_3 and WO_3. The calculated energy of L-MoO_3 includes an estimate for electron correlation in the interlayer binding; the fully optimised Hex-WO_3 phase includes off-centerings of the W ions along the axial direction, without long-range order in the structure [50]. The bottom part of the table refers to structures optimised with the M ions on-centre in their coordination octahedra, and applies to the relative stability of the MO_3 frameworks in the bronzes.

The calculated energies reported in the bottom part of Table 1 give therefore, the relative stability of the MO_3 framework of MoO_3 and WO_3 in the insertion compounds.

The interaction of the MO_3 backbone with the extraframework ions A^+ provides an additional contribution to the relative stability of the polymorphs, which again can be estimated via computer modelling. In [51], we have compared the migration profile of Na^+ and K^+ ions in the hexagonal tungsten bronzes $A_{1/3}WO_3$; a calculated difference of 0.52 eV per inserted ion, in the interstitial position closest to the framework oxygens, is associated with the different ionic dimensions of Na^+ and K^+. The latter value provides an estimate for the short-range repulsion energy between the host framework and each inserted K^+ ion. The steric repulsion energy between the host transition metal oxide framework and the extraframework species, can be assumed to be proportional to the size of the latter, and can be varied via the addition of different-sized extraframework ions to the synthesis medium. The value of 0.52 eV, calculated for the K^+ ion, is comparable to the calculated energy difference between the PV, Hex and PY frameworks; the short-range repulsion between framework and inserted ions plays therefore, a relevant role in the energetics of the bronzes, and may reverse the relative stability of different framework structures. This is confirmed by the experimentally reported crystal structures of the W bronzes: increasing the size of the extraframework ions we move from the cubic perovskite form of $NaWO_3$ towards the hexagonal K_xWO_3 and Rb_xWO_3, to the pyrochlore structure obtained by insertion of Cs and of primary and secondary ammonium salts. The latter comparison suggests that if the extraframework ions are present during the synthesis, the energy arising from the short-range repulsion is sufficient to offset the energy difference between the polymorphic struc-

tures, and to shift the stability towards the polymorphs with the appropriate interstitial dimensions. We can in such a case identify the extraframework ions as inorganic templates, or structure-directing agents, for the forming MO_3 frameworks.

What happens if we increase the size of the extraframework ions, so that the steric repulsion between framework and inserted ions becomes the prevailing force during the synthesis? Among inorganic species, the range of ionic dimensions achievable to modulate the steric interaction energy is limited, and the alkali ions referred to above are already those with the largest ionic radius. Larger stable ions can however, be easily found among organic molecules, and metallo-organic complexes.

The template/host relation between extraframework ions and transition metal oxide structure, recalls similar fields of research; the use of organic cationic templates, for instance, is the standard procedure in the synthesis of microporous alumino-silicates (zeolites), which heavily relies on the presence of organic cations in the synthesis medium, to create molecular-sized interstices in the forming SiO_2 structure. The correlation between the shape of the organic cation and that of the micropores obtained in the zeolitic material is now recognised [52–55]. Space-filling approaches are also adopted in the synthesis of pillared catalysts, such as clays [56], and even of molecular crystals (clathrates) [57].

Attempts to use larger organic cations, usually quaternary ammonium salts, to template novel transition metal oxide frameworks have already been reported in the literature [45,58]. However, they resulted in the formation of inorganic polyanions, the Keggin structures, rather than extensive M–O frameworks. In the following discussion, we shall examine the topic with a more analytic approach, exploiting the insight that can be obtained from computer modelling to provide information on the relative stability and on the required synthesis conditions for new, microporous structures of transition metal oxides. If the pore sizes reach the dimension of small organic molecules, and provided the new frameworks have sufficient stability at high temperatures, microporous transition metal oxides would allow heterogeneous catalytic applications. Synthesising novel materials that could combine the molecular-sieve characteristics of zeolites, with the much higher acidic strength and redox properties of early transition metal cations, would indeed be a major breakthrough in catalysis. Of course, this is a very challenging task, since microporous structures of MoO_3 and WO_3 have so far never been reported.

Before proceeding, it is instructive to extend the comparison with zeolites, and examine the computational procedures that have recently been developed to understand and guide the synthesis of microporous structures. We shall then transfer the relevant knowledge to the new field of microporous transition metal oxides.

4.1. Analogy with zeolites

Zeolites are polymorphs of silica, of stoichiometry SiO_2, with an open framework structure. The framework cations are tetrahedrally coordinated by four nearest neighbour oxygens.

In the pure SiO_2 form, or when Si is replaced by stoichiometric amounts of $+3$ and $+5$ ions such as Al and P, the zeolitic framework is chemically inert. If, however, a charge imbalance occurs in the framework, for instance by replacing a Si^{4+} cation with Al^{3+}, the framework is chemically activated. The overall negative charge of the tetrahedral backbone is compensated during the synthesis by the extraframework cations, the same acting as templates. The extraframework cations can be exchanged with protons in post-synthetic treatments, yielding Brønsted acid sites in the solid. Al-doped zeolites are used in a range of acid-activated heterogeneous catalytic reactions.

The most attractive features of microporous solids as heterogeneous catalysts are those of having high surface areas per unit of weight (in fact the whole of the solid can be imagined as a single three-dimensional surface), and of containing the active sites in a spacially confined environment, where they can be accessed only by selected molecules and/or parts of molecules, leading to a highly specific shape-selectivity in the reactions catalysed [59].

Zeolites are thermodynamically unstable compared to the α-quartz structure of SiO_2; the topic is examined with the same computational technique employed here in a recent paper [60]. The energy difference between the silica polymorphs is in the range of $\simeq 0.1$–0.2 eV per formula unit, much smaller than the one we calculated for MoO_3 and WO_3; excluding the L polymorph, the energy range of the PV, Hex and PY structures is

in fact of $\simeq 0.5$ eV per formula unit. We attribute the higher energy difference in the Mo and W trioxides to two effects:

1. the higher ionic charges, which increases the Madelung field, and hence the energy toll to pay when the density of the solid is decreased by introducing larger interstices; and
2. the rigidity of the octahedral framework of transition metal oxides, compared to the more flexible tetrahedral framework of silicates, whose Si–O (or Al–O) backbone is formed only by σ bonds. The σ bonds allow in fact an easy rotation of the structure along the M–O direction, with small energy barriers, to respond to local strains. The flexibility of the O–Si–O, and especially of the Si–O–Si angles in zeolites is confirmed by the wide range of values observed, which covers almost all values between 90 and 180°. In comparison, the π frontier orbitals in early transition metal oxides, confer rotational rigidity to the M–O bonding, which can less easily adapt to local strains.

The difference in framework energy between the polymorphs examined of MoO_3 and WO_3, however, is still in the range of energy provided by the steric repulsion, and can be reversed, as confirmed by the different stable structures of the alkali W bronzes.

A computational strategy has been recently developed for the de novo design of structure-directing agents in zeolites [61], and implemented in a computer code, ZEBEDDE [62]. Given a target microporous architecture, the organic template is gradually grown computationally within the pores of the host, starting from a small molecular fragment used as seed. The implementation in ZEBEDDE employs a cost-function approach to construct molecules that best fill the void space of the targeted crystalline host. The cost-function can either be based on a sum of close contacts between atoms in template and host, or on the interaction energy between the two, calculated via interatomic potentials. In the latter case, repulsion and dispersion forces are summed up to a user-defined cut-off, and the electrostatic contribution to the energy is calculated using Ewald summations.

Optimal space-filling is achieved by growing the template molecules within the porous host; at each stage of the tentative template construction, the position, orientation and configuration of the molecule is altered, to minimise the cost-function, and hence maximise its interaction energy with the host. The technique generates, in this way, a set of organic templates which are likely to provide optimal space-filling and/or maximum interaction energy with the selected microporous host, thus helping to direct the synthesis towards the target structure.

4.2. Microporous transition metal oxides

The method implemented in the code ZEBEDDE, requires the knowledge of the porous structure as a starting point. When transferred to transition metal oxides, this is a challenging task by itself, since microporous structures built up only on MO_6 octahedra have so far never been reported. The only exception are the OMS sieves based on edge-sharing of $Mn^{IV}O_6$ units [63–65], in which the framework has stoichiometry MO_2 and not MO_3 as required for the Mo and W oxides. The first problem to solve is therefore, that of designing a suitable target structure.

The stability requirements, as can be deduced from the structure of the stable Mo and W bronzes, are that each oxygen ion be shared between at least two neighbouring M ions, avoiding 1-coordinate oxygens which would break the framework connectivity, as in the L polymorph. The structure must also contain the maximum extent of corner-sharing of octahedra, which is stable upon insertion of extraframework ions and reduction of the host transition metal cations.

The design of new polymorphs can be reformulated as a problem of tiling in space. If we connect the M ions along corner-shared octahedra in the PV, Hex and PY polymorphs, we obtain a tiling based on adjoining triangles, squares and hexagons. No other polygon allows a complete space-filling under the constraint of periodic boundary conditions necessary to yield crystalline materials, and the PV, Hex and PY structures exhaust the possibilities based on corner-sharing only of single octahedral units. In the new structures we need therefore, to introduce some extent of edge-sharing between octahedra. The PV and Hex structures can be further imagined as a two-dimensional tiling, repeated by corner-sharing of the axial oxygens along the third (c) crystallographic direction. In the design of new structures, we shall retain this two-dimensional approach, as a useful starting point to assess the feasibility of the method.

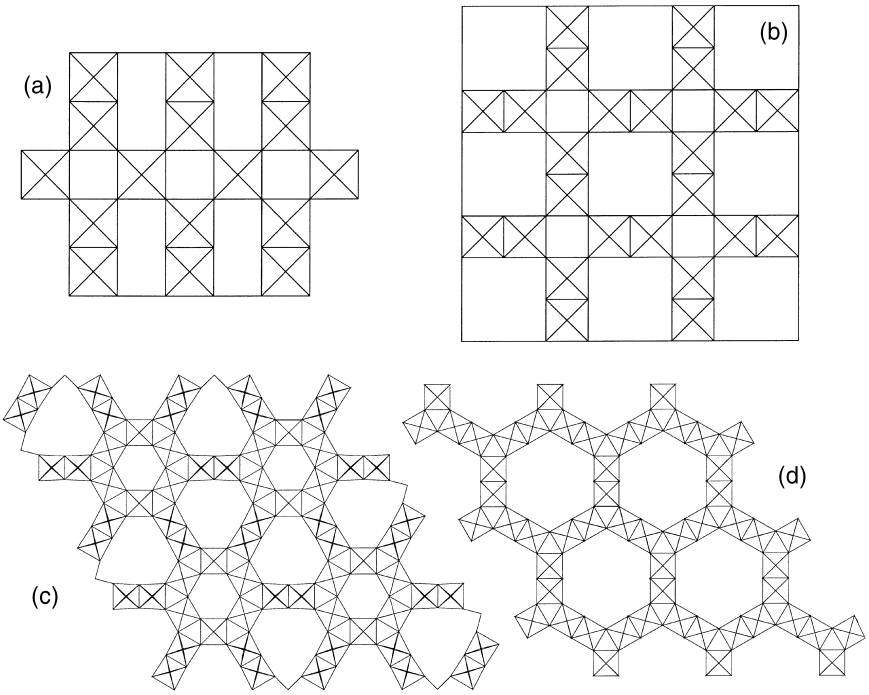

Fig. 2. Disposition of octahedra in the MO_3 framework of the: (a) $PV^{2\times1}$; (b) $PV^{2\times2}$; (c) $H^{2\times1}$; (d) $H^{2\times2}$ microporous structures.

We have devised two ways of proceeding.

1. If we define a new building block, as a chain of *n* aligned edge-shared octahedra, a complete series of new structures can be obtained from the same two-dimensional tiling of the PV and Hex phases, using tiles with sides of different length, for instance with polygons whose sides have alternating lengths of *m* and *n* units (in the case examined, chains of *m* and *n* edge-shared octahedra).

   Given the method of construction, we call the new structures $PV^{m\times n}$ and $H^{m\times n}$ (the 1×1 structures reproduce the PV and Hex polymorphs). A schematic representation of the first members of the $H^{m\times n}$ and $PV^{m\times n}$ series is reported in Fig. 2.
2. Alternatively, microporous structures can be derived from a projection of the Hex polymorph onto the crystallographic *ab* plane, according to the method exemplified in Fig. 3. In the first step (Fig. 3b), one or more octahedra (squares in the two-dimensional projection) are subtracted, to form an hexagonal super-lattice with missing octahedral blocks; the octahedra deleted are those enclosed in the bold triangles in Fig. 3b. The subtraction leads to the microporous super-lattices represented in Fig. 3c. In the second step, the vertices left 1-coordinated by the first operation are merged, to form edge-shared octahedra; the chains of edge-shared octahedra are represented by the shaded area in Fig. 3d.

   The $H^{m\times n}$ structures can be reproduced with this second procedure, which is therefore, more general for designing microporous structures related to the Hex polymorph; it cannot however, be applied to the PV lattice. The case in which the second method yields the $H^{2\times2}$ polymorph is shown in the left column of Fig. 3; the structure in the right column cannot instead be obtained via the first route.

The structures obtained with either of the above methods have MO_3 framework stoichiometry. In this respect, they are equivalent to the pure SiO_2 form of zeolites. As in zeolites, charge imbalances can be introduced into the MO_3 framework by chemical doping, for instance by replacing the host Mo^{6+} or W^{6+} cations with a group-V ion, such as V^{5+}, Nb^{5+} or

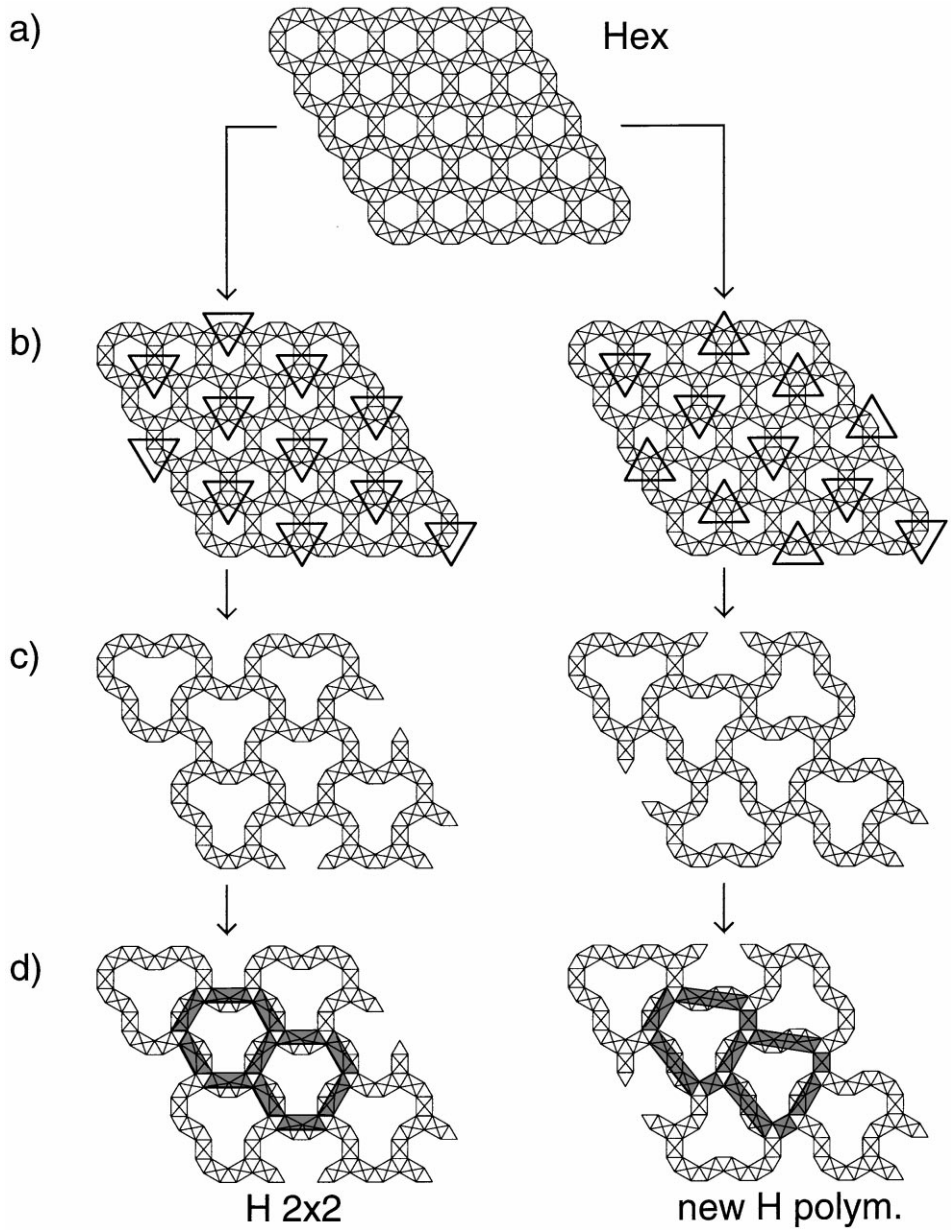

Fig. 3. Construction of microporous MO_3 structures by creating a super-lattice of missing octahedral blocks in the parent Hex-MO_3 structure.

Ta^{5+}. The latter operation is equivalent to the creation of Brønsted acid sites in zeolites by the doping with Al^{3+} ions. Such chemistry, however, is not examined here; in this initial stage, we are only concerned with the stability of the unsubstituted microporous MO_3 frameworks. It is important to mention, however, that the transition metal ions examined (Mo and W) have by themselves a redox ability, and can therefore, accommodate the presence of extraframework cations by reducing their oxidation state, as in the alkali bronzes

examined earlier. Both neutral and cationic templates can therefore, be employed in the synthesis of the porous transition metal oxides. In zeolites, on the contrary, the presence of charged cationic templates during the synthesis, must be charge-compensated with the introduction of a sufficient amount of Al^{3+} ions in the backbone.

We have calculated the electronic distribution, geometry and energy of first two members, the 2×1 and 2×2, of the $H^{m\times n}$ and $PV^{m\times n}$ series, for both compositions MoO_3 and WO_3. In all cases, the structure has been optimised under the constraint of keeping the transition metal ions on-centre in their coordination octahedra. If, as for the zeolites, cationic templates are used in the synthesis, the transition metals will be in a reduced state; we have therefore, excluded the chemical distortions of the MO_6 octahedra from the energy minimisation, but allowed the lattice parameters and the internal coordinates of the M and O ions to relax fully under the local Coulomb field generated by the neighbouring ions.

All the new structures examined represent local minima in the potential energy surface; hence, if synthesised, they would have a non-zero activation barrier towards phase transformations, and may be kinetically stable.

The calculated internal energy of the MO_3 framework in the microporous polymorphs is compared in Table 1 with that of the known structures. The microporous polymorphs are unstable, as expected; the energy difference, however, is still comparable with that among the known polymorphs, and has only a marginally larger magnitude than the steric forces examined earlier. We consider it to be possible to overcome this energy difference with steric effects. Given the relative instability of the framework, the template must however, be selected very carefully, and must fit very tightly in the porous structure to stabilise the new polymorphs, which is probably why previous attempts with randomly selected organic templates have failed. The search for templating molecules with the required features may achieve a much higher accuracy by applying the computational method devised for the synthesis of zeolites.

As a final step in the computational procedure, we have applied the de novo method to design templating agents specific for the $H^{2\times1}$ and $H^{2\times2}$ structures, those whose interstices are more likely to accommodate organic ions.

The implementation of the method in the code ZEBEDDE is based on interatomic potentials. In previous applications to the growth of templates for zeolitic frameworks [61], all interactions were described by a consistent set of interatomic potentials, both the intra-framework Si–O and the template-framework forces. The electrons populating the σ Si–O bonds that compose the silica backbone of zeolites are localised in the structure between the bonded atomic pair, and the σ Si–O bonds are well characterised chemically; they are therefore, suitable for a description with interatomic potentials, to take into account the local constraints imposed by the surrounding lattice. Sets of parameters derived to describe SiO_2 polymorphs are available in the literature [66–70]. In the case of zeolites, the relaxation of the SiO_2 framework structure around the tentative template molecule was therefore, included consistently in the computational method. This is not the case, however, for transition metal oxides, in which structural distortions cause extensive rehybridisations of the frontier π M–O levels, whose bonding, non-bonding or antibonding character is subject to symmetry constraints of quantum-mechanical nature [49]. Deriving a set of interatomic potentials to describe the MO_3 framework would represent a crude approximation. On the other hand, the estimate of interactions via interatomic potentials describes with sufficient accuracy the two-body repulsion forces at the basis of the steric, templating effect of the extraframework ions. For this reason, we have employed a two-step procedure in the template construction. First, we have optimised the host MO_3 framework with QM methods which correctly represent the M–O bonding. Second, the framework structure is fixed at its energy-minimised geometry, and the template is grown in the pores of the host. During this second step, the host geometry is not allowed to change; energy-minimised structures have been obtained by relaxing only the template molecule, at each stage of its growth.

The steric interactions between the MO_3 framework and the organic template have been evaluated with the same set of interatomic potentials used for zeolites [70], including the term between framework oxygens and organic molecule, but ignoring the M-template

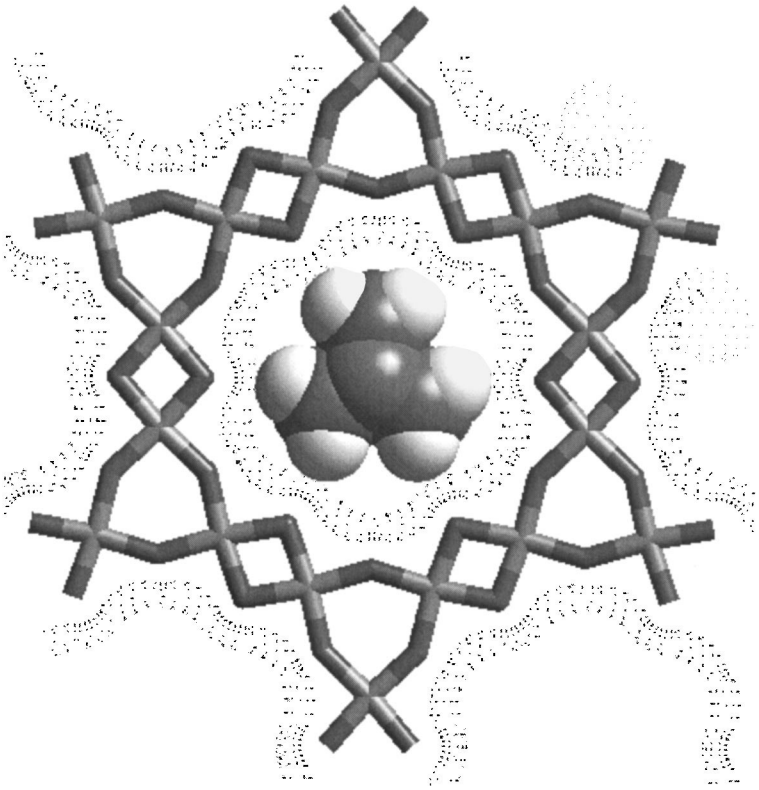

Fig. 4. Di-azobicyclooctane (DABCO) molecule, as located by the code ZEBEDDE inside the pores of the $H^{2\times2}$ polymorph. The darker atoms in the framework are oxygens; the lighter atoms the transition metals. The shaded surface represents the solvent-accessible surface inside the pores, and renders the volume occupied by the framework oxygens.

short-range interaction potential. The latter appears however, a good approximation, as the shape of the pores is controlled by the oxygens and not by the M ions of the structure. The effect of the transition metal ions was instead included in the electrostatic field, by attributing to them the net charges calculated at the QM level via a Mulliken population analysis of the electronic distribution.

The candidate template molecules obtained by the use of ZEBEDDE have been ranked by their calculated binding energy (E_B) with the host lattice: the higher E_B, the more favourable the molecule is considered as a template [53]. The calculations performed reveal that the pores of the $H^{2\times1}$ structure have dimensions comparable to unsubstituted hydrocarbon chains, suggesting that *N*-amines or *N*-diamines, as used in zeolite synthesis, may be suitable as templates. The pores of the $H^{2\times2}$ polymorph have instead a size comparable to the 12-membered rings in zeotypes, and allow the insertion of more structured organic moieties. The calculations reveal that adamantane and di-azobicyclooctane (DABCO) derivatives are of suitable dimensions, the latter being the most promising. A picture of the DABCO template, as located by the code ZEBEDDE inside the pores of the $H^{2\times2}$ polymorph of WO_3, is reported in Fig. 4. It is interesting to note there the match between the six-fold symmetry of the porous $H^{2\times2}$ structure and the six hydrogen atoms of the DABCO organic template. The shaded surface in Fig. 4 represents the solvent-accessible surface inside the pores, and renders the volume occupied by the framework oxygens. Each hydrogen of the template is in close, 1:1, correspondence with one framework oxygen, suggesting that a strong stabilisation from hydrogen bonding may arise in such a configuration.

5. Conclusions

We have employed periodic ab initio HF calculations to examine the relative stability and electronic properties of the Mo and W trioxides, and how they are modified during the insertion process that leads to the formation of the bronzes A_xMO_3.

Extraframework ions show a templating effect towards the stable structure of the host transition metal oxide framework, which may be exploited for the synthesis of novel polymorphs. We have examined the latter topic by designing new microporous structures of MoO_3 and WO_3, and exploring the feasibility of their synthesis, employing modelling in advance experiment.

We consider that the computational study presented here shows the feasibility on energetics grounds of an extensive range of microporous chemistry based on octahedral MoO_3 and WO_3, and suggests that such structures may be synthesised using a host/guest templating approach. Future experimental studies will test the prediction of these calculations. If successful, it would be the first time that a new solid catalyst has been derived completely on theoretical grounds, from its design stage, up to the 'recipe' for its synthesis, a target that computer modelling should pose itself in future advanced applications.

Acknowledgements

EPSRC is gratefully acknowledged for funding this research project and for the provision of time on the IBM/SP2 computer at the Daresbury Laboratory.

References

[1] D.H. Dawson, D.E. Williams, J. Mater. Chem. 6 (1996) 409.
[2] H.H. Kung, Surface Chemistry and Catalysis of Transition Metal Oxides, Elsevier, Amsterdam, 1989.
[3] V.E. Heinrich, P.A. Cox, The Surface Science of Metal Oxides, Cambridge University Press, Cambridge, 1994.
[4] M. Green, Chem. Ind. 17 (1996) 641.
[5] R.J. Mortimer, Chem. Soc. Rev. 26 (1997) 147.
[6] K.H. Yoon, J.W. Lee, Y.S. Cho, D.H. Kang, J. Appl. Phys. 80 (1996) 6813.
[7] J.R. Owen, Chem. Soc. Rev. 26 (1997) 259.
[8] Lithium batteries, Pistoia (Ed.), Elsevier, Amsterdam, 1994.
[9] C. Pisani, R. Dovesi, C. Roetti, Hartree-Fock Ab Initio Treatment of Crystalline Systems, Lecture Notes in Chemistry, Vol. 48, Springer, Heidelberg, 1988.
[10] V.R. Saunders, R. Dovesi, C. Roetti, M.Causà, N.M. Harrison, R. Orlando, C.M. Zicovich-Wilson, CRYSTAL 98 User's Manual, University of Torino, Italy, Turin, 1998.
[11] P.J. Hay, W.R. Wadt, J. Chem. Phys. 82 (1985) 270, 284, 299.
[12] F. Corà, A. Patel, N.M. Harrison, C. Roetti, C.R.A. Catlow, J. Mater. Chem. 7 (1997) 959.
[13] F. Corà, A. Patel, N.M. Harrison, R. Dovesi, C.R.A. Catlow, J. Am. Chem. Soc. 118 (1996) 12174.
[14] W.L. Kehl, R.G. Hay, D. Wahl, J. Appl. Phys. 23 (1952) 212.
[15] J. Wyart, M. Foex, C.R. Acad. Sci. 233 (1951) 2459.
[16] E. Salje, Acta Cryst. B 33 (1977) 574.
[17] B.O. Loopstra, P. Boldrini, Acta Cryst. 21 (1966) 158.
[18] E. Salje, K. Viswanathan, Acta. Cryst. B 31 (1975) 356.
[19] R. Diehl, G. Brandt, E. Salje, Acta Cryst. B 34 (1978) 1105.
[20] E.M. McCarron, Chem. Commun. 336 (1986).
[21] J.B. Parise, E.M. McCarron, R. von Dreele, J. Solid State Chem. 93 (1991) 193.
[22] P.G. Dickens, D.J. Neild, Trans. Faraday Soc. 64 (1968) 13.
[23] N.C. Stephenson, A.D. Wadsley, Acta Cryst. 19 (1965) 241.
[24] J. Graham, A.D. Wadsley, Acta Cryst. 20 (1966) 93.
[25] M. Figlarz, Prog. Solid State Chem. 19 (1989) 1.
[26] T. Nanba, I. Yasui, J. Solid State Chem. 83 (1989) 304.
[27] T. Nanba, Y. Nishiyama, I. Yasui, J. Mater. Res. 6 (1991) 1324.
[28] T. Nanba, T. Takahashi, S. Takano, J. Takada, A. Osaka, Y. Miura, T. Kudo, I. Yasui, J. Ceram. Soc. Jpn. 103 (1995) 222.
[29] B. Gerand, G. Nowogrocki, J. Guenot, M. Figlarz, J. Solid State Chem. 29 (1979) 429.
[30] I.P. Olenkova, L.M. Plyasova, S.D. Kirik, Reaction Kinetics Catal. Lett. 16 (1981) 81.
[31] J.D. Guo, P. Zavalij, M.S. Whittingham, European J. Solid State Inorg. Chem. 31 (1994) 833.
[32] J.D. Guo, P. Zavalij, M.S. Whittingham, J. Solid State Chem. 117 (1995) 323.
[33] N.A. Caiger, S. Crouchbaker, P.G. Dickens, G.S. James, J. Solid State Chem. 67 (1987) 369.
[34] C. Gemin, A. Driouiche, B. Gerand, M. Figlarz, Sol. St. Ionics 53-6 (1992) 315.
[35] T. Kudo, J. Oi, A. Kishimoto, M. Hiratani, Mater. Res. Bull. 26 (1991) 779.
[36] A. Driouiche, F. Abraham, M. Toubol, M. Figlarz, Mater. Res. Bull. 26 (1991) 901.
[37] A.B. Swanson, J.S. Anderson, Mater. Res. Bull. 3 (1968) 149.
[38] P.J. Wiseman, P.G. Dickens, J. Solid State Chem. 17 (1976) 91.
[39] P.J. Wiseman, P.G. Dickens, J. Solid State Chem. 6 (1973) 374.
[40] I. Tsuyumoto, A. Kishimoto, T. Kudo, Sol. St. Ionics 59 (1993) 211.
[41] H. Prinz, U. Müller, M.L. Haeierdanz, Z. Anorg. Allg. Chem. 609 (1992) 95.
[42] R.C.T. Slade, P.R. Hirst, B.C. West, J. Mater. Chem. 1 (1991) 281.
[43] Q.M. Zhong, W. Colbow, Thin Solid Films 196 (1991) 305.

[44] J.D. Guo, K.P. Reis, M.S. Whittingham, Sol. St. Ionics 53-6 (1992) 305.
[45] P. Zavalij, J.D. Guo, M.S. Whittingham, R.A. Jacobson, V. Pecharsky, C.K. Bucker, S.J.H. Wu, J. Solid State Chem. 123 (1996) 83.
[46] N.C. Stephenson, Acta Cryst. 20 (1966) 59.
[47] E. Canadell, M.H. Whangbo, Chem. Rev. 91 (1991) 965.
[48] F. Corà, M. Stachiotti, C.O. Rodriguez, C.R.A. Catlow, J. Phys. Chem. B 101 (1997) 3945.
[49] F. Corà, C.R.A.Catlow, Faraday Discussions 114 (1999) 221.
[50] F. Corà, Ph.D. Thesis, The Royal Institution of Great Britain and the University of Portsmouth, 1999.
[51] F. Corà, C.R.A. Catlow, Sol. St. Ionics 112 (1998) 131.
[52] M.E. Davis, R.F. Lobo, Chem. Mater. 4 (1992) 759.
[53] D.W. Lewis, C.M. Freeman, C.R.A. Catlow, J. Phys. Chem. 99 (1995) 11194.
[54] A.P. Stevens, A.M. Gorman, C.M. Freeman, P.A. Cox, J. Chem. Soc., Farad. Trans. 92 (1996) 2065.
[55] R.E. Boyett, A.P. Stevens, M.G. Ford, P.A. Cox, Zeolites 17 (1996) 508.
[56] R.J.M.J. Vogels, M.J.H.V. Kerkhoffs, J.W. Geus, Stud. Surf. Sci. Catal. 91 (1995) 1153.
[57] M. Ward, Chem. Br. (1998) 52–56.
[58] G.G. Janauer, A. Dobley, J.D. Guo, P. Zavalij, M.S. Whittingham, Chem. Mater. 8 (1996) 2096.
[59] J.M. Thomas, Sci. Am. 267 (1992) 12.
[60] B. Civalleri, C.M. Zicovich-Wilson, P. Ugliengo, V.R. Saunders, R. Dovesi, Chem. Phys. Lett. 292 (1998) 384.
[61] D.W. Lewis, D.J. Willock, C.R.A. Catlow, J.M. Thomas, G.J. Hutchings, Nature 382 (1996) 604.
[62] D.W. Lewis, D.J. Willock, Code ZEBEDDE, ZEolites By Evolutionary De-novo DEsign, 1996–1998.
[63] Y.F. Shen, S.L. Suib, C.L. Oyoung, J. Am. Chem. Soc. 116 (1994) 11020.
[64] Y.F. Shen, R.N. Deguzman, R.P. Zerger, S.L. Suib, C.L. Oyoung, Stud. Surf. Sci. Catal. 83 (1994) 19.
[65] S.R. Wasserman, K.A. Carrado, S.E. Yuchs, Y.F. Shen, H. Cao, S.L. Suib, Physica B 209 (1995) 674.
[66] R.A. Jackson, C.R.A. Catlow, Mol. Simul. 1 (1988) 207.
[67] J.-R. Hill, J. Sauer, J. Phys. Chem. 98 (1994) 1238.
[68] J.-R. Hill, J. Sauer, J. Phys. Chem. 99 (1995) 9536.
[69] K.-P. Schröder, J. Sauer, J. Phys. Chem. 100 (1996) 11043.
[70] cff91-czeo Molecular Forcefield and Discover 4.0, Molecular Simulation Inc., San Diego, 1997.